

1 Prediction of the sweetening effect of *Siraitia grosvenorii* (luo  
2 han guo) fruits by two-dimensional quantitative NMR

3

4

5 Serhat S. Çiçek<sup>a,\*</sup>, Tiffany Esposito<sup>a</sup>, Ulrich Girreser<sup>b</sup>

6

7

8 <sup>a</sup> Pharmazeutisches Institut, Abteilung Pharmazeutische Biologie, Christian-Albrechts-  
9 Universität zu Kiel, Gutenbergstraße 76, 24118 Kiel, Germany

10

11 <sup>b</sup> Pharmazeutisches Institut, Abteilung Pharmazeutische und Medizinische Chemie, Christian-  
12 Albrechts-Universität zu Kiel, Gutenbergstraße 76, 24118 Kiel, Germany

13

14 \* Corresponding author. *E-mail address*: [scicek@pharmazie.uni-kiel.de](mailto:scicek@pharmazie.uni-kiel.de)

15

16 **ABSTRACT**

17

18 During the last decade, dried fruits of *Siraitia grosvenorii* (luo han guo), also known as monk  
19 fruit, have become popular food ingredients. Luo han guo extracts, which are promoted as non-  
20 caloric natural sweeteners, are now incorporated into dietary supplements, soft drinks, and  
21 energy shakes. The compounds responsible for the sweetening effect are glycosylated  
22 cucurbitane-type triterpenoids, the so-called mogrosides. However, of the more than 40 known  
23 mogroside compounds, only 11- $\alpha$ -hydroxy-mogrosides exhibit a sweetening effect, whereas the  
24 other triterpenoids are non- or bitter-tasting. We have used two-dimensional quantitative NMR  
25 to determine selectively the content of 11- $\alpha$ -hydroxy-mogrosides in these dried fruits and thus  
26 to predict their sweetening potential. Homonuclear (H,H COSY) and heteronuclear (HSQC)  
27 methods were developed, validated, and compared. Both techniques were found suitable for the  
28 quality control of luo han guo fruits and extracts, the COSY experiment being advantageous  
29 with regard to accuracy, precision, and limit of quantification.

30

31

32 **Keywords:** *Siraitia grosvenorii*; Cucurbitaceae; luo han guo; mogrosides; HSQC; COSY;  
33 qNMR; natural sweetener

## 34 1. Introduction

35

36 *Siraitia grosvenorii* (Swingle) C.Jeffrey ex A.M.Lu & Zhi Y.Zhang, also referred to as  
37 *Momordica grosvenorii* or *Thladiantha grosvenorii*, is a perennial vine of the Cucurbitaceae  
38 family (Pawar, Krynitsky, & Rader, 2016). Commonly known as “monk fruit” or “luo han guo”,  
39 *S. grosvenorii* is native to the southern part of China, where it has been used as a food ingredient  
40 and herbal medicine for more than 300 years (Gong et al., 2019; Soejarto, Addo, & Kinghorn,  
41 2019). *S. grosvenorii* is applied in typical ethnomedical treatments of ailments such as coughs,  
42 lung congestion, and sore throats and was one of the first food homology species approved for  
43 medical use in China (Gong et al., 2019). The plant was listed as a medicinal and edible species  
44 by the China Ministry of Health in 1987 (Li et al., 2014). In the 1990s, the China Food and  
45 Drug Administration approved luo han guo as a food sweetener and as a substitute for  
46 sweeteners in health foods for patients with obesity and diabetes. Preparations of the dried fruits  
47 have subsequently been marketed as sugar-free food additives and used in low-calorie health-  
48 promoting juices. Since 2011, extracts and preparations of *S. grosvenorii* have become  
49 commercially available in the United States and are currently produced at large scale for  
50 utilization as table-top sweeteners (Fletcher, Pan, & Kinghorn, 2017; Pawar et al., 2016).  
51 Having been awarded the GRAS (“generally regarded as safe”) status in the U.S., *S. grosvenorii*  
52 can now be considered the most popular natural sweetener after *Stevia rebaudiana* (Soejarto et  
53 al., 2019).

54 Like that of *S. rebaudiana*, the sweetening effect of *S. grosvenorii* constituents is reported  
55 to be up to 500 times as high as that of sucrose (Li et al., 2014; Pawar et al., 2016; Soejarto et  
56 al., 2019). However, in contrast to the sweet-tasting diterpenoids contained in stevia, the  
57 compounds responsible for the sweetening effect of luo han guo are glycosylated cucurbitane-  
58 type triterpenes. These compounds are characterized by a four-ring scaffold and various sugar

59 moieties at position C-3 and C-24 (Fig. 1). The major sugar present in mogrosides is D-glucose,  
60 although L-rhamnose moieties have also been reported (Qing et al., 2017). The number of  
61 attached glucose units is expressed by Roman numerals in the compound name (rhamnoses are  
62 indicated separately), with a reported maximum of seven sugar moieties (Qing et al., 2017).  
63 Depending on the nature of position C-11, which can be a carbonyl group, a methylene group,  
64 or an  $\alpha$ -hydroxy-methine group, in the scaffold, the compounds are referred to as 11-oxo-  
65 mogrosides (**1**), 11-deoxymogrosides (**4**), or mogrosides (**2** and **3**). The last-mentioned term is  
66 also used to circumscribe all of the luohanguo triterpenoids, however, only mogrosides with  
67 the mogrol aglycone (**2** and **3**) possess the sweet taste. This means that the  $\alpha$ -hydroxy-group is  
68 crucial for the sweetness effect, as is the presence of at least three glucose moieties (Li et al.,  
69 2014).

70 So far, more than 40 cucurbitane-type triterpenoids have been isolated from *S. grosvenorii*,  
71 of which 17 show the features necessary for exhibiting a sweet taste (Çiçek, 2020). With regard  
72 to the biosynthesis of mogrosides, the glucose moieties are successively attached to the  
73 aglycone during the ripening process. Mogroside V (**3**), the major triterpenoid, appears  
74 approximately 50 days after flowering and peaks after 70 days, whereas the mogroside IV class  
75 peaks as early as 40 days after flowering (Itkin et al., 2016; Pawar et al., 2016; Qing et al.,  
76 2017). Because of these variations over time and the overall complexity of the constituent  
77 pattern, quantitative (chromatographic) methods for the quality control of luohanguo have  
78 focused on one mogroside, namely mogroside V (**3**) (Deng, Liang, Yang, Liu, & Liu, 2013;  
79 Makapugay, Nanayakkara, Soejarto, & Kinghorn, 1985) or a few constituents (Li et al., 2007;  
80 Luo, Shi, Zhang, Qin, Guo, & Ma, 2016; Shen et al., 2014). In these studies, the amount of  
81 mogroside V (**3**) has been found to vary between 5.8 and 12.9 mg/g dry fruit, whereas the  
82 cumulated content of the major compounds has been reported to be between 8.8 and 18.5 mg/g  
83 (Luo et al., 2016; Makpugay et al., 1985; Shen et al., 2014). This contrasts with results obtained

84 from a colorimetric assay, which has determined the total content of mogrosides as being 38.2  
85 mg/g dry fruit (Li et al., 2014). However, neither colorimetric nor chromatographic methods  
86 have so far accomplished a determination of the total amount of 11- $\alpha$ -hydroxy-mogrosides or  
87 an analysis of the sweetening potential of luo han guo at a molecular level.

88 In the present work, we investigated the fruits of *S. grosvenorii* with two-dimensional NMR  
89 spectroscopy by using its characteristic measuring principle, the detection of specific structural  
90 features. We hypothesized that signals exclusively resulting from 11- $\alpha$ -hydroxy-mogrosides  
91 could be used for the quantification of this particular compound class. This strategy should  
92 allow the selective determination of the compounds of interest and consequently the prediction  
93 of the sweetening effect of the ripe fruits.

94

## 95 **2. Materials and methods**

96

### 97 *2.1. Plant material and chemical reagents*

98

99 Dried fruits of *Siraitia grosvenorii* (Golden Diamond, Lot B02/2549) were obtained from  
100 the Go Asia supermarket (Hamburg, Germany). 1,2,4,5-Tetrachloro-3-nitrobenzene TraceCert  
101 for quantitative NMR (Lot BCBR7216V, 99.86%), LC-MS grade formic acid, Diaion HP-20,  
102 and Sephadex LH-20 were purchased from Sigma Aldrich Co., St. Louis, MO, USA. Silica gel  
103 (40-63  $\mu$ m) for column chromatography, TLC plates (silica gel 60 F<sub>254</sub>), acetonitrile and water  
104 (both of LC-MS grade), gradient grade methanol, and other (analytical grade) solvents were  
105 obtained from VWR International GmbH, Darmstadt, Germany. Water used for isolation was  
106 doubly distilled in-house. Solid phase extraction (SPE) columns (Chromabond SB 3 mL/500  
107 mg, Chromabond C18 6 ml/1000 mg) were obtained from Macherey-Nagel GmbH and Co. KG,  
108 Düren, Germany. Dimethyl sulfoxide-*d*<sub>6</sub> (99.80%, Lot S1051, Batch 0119E) and pyridine-*d*<sub>5</sub>

109 (99.50%, Lot Q1301, Batch 1116) for NMR spectroscopy were purchased from Euriso-top  
110 GmbH, Saarbrücken, Germany, and conventional 5 mm NMR sample tubes were obtained from  
111 Rototec-Spintec GmbH, Griesheim, Germany.

112

## 113 *2.2. General experimental procedures*

114

115 Thin layer chromatography was performed using *n*-butanol–ethanol–water (40–10–15) as  
116 the eluent and vanillin sulfuric acid as the spraying reagent. Flash chromatography was carried  
117 out with a Buchi PrepChrom C-700 chromatograph and FlashPure Ecoflex (50 µm irregular,  
118 10 g) silica gel cartridges (Büchi Labortechnik GmbH, Essen, Germany). Preparative MPLC  
119 was performed with the same instrument but by using a Buchi PrepChrom C18 column (250 ×  
120 30.0 mm, 15 µm particle size). Semi-preparative HPLC was accomplished using a Waters  
121 Alliance e2695 Separations Module with an Alliance 2998 photodiode array, and a WFC III  
122 fraction collector (Waters, Milford, MA, USA) using a VP Nucleodur C18 column (250 × 10  
123 mm, 5 µm particle size, Macherey-Nagel GmbH and Co. KG, Düren, Germany). UHPLC  
124 analyses were performed on a VWR-Hitachi Chromaster Ultra RS equipped with a 6170 binary  
125 pump, 6270 autosampler, 6310 column oven, 6430 DAD, and VWR 100 evaporative light  
126 scattering detector (VWR International GmbH, Darmstadt, Germany). LC-MS analyses were  
127 carried out on a Shimadzu Nexera 2 liquid chromatograph connected to an LC-MS triple  
128 quadrupole mass spectrometer using electrospray ionization (Shimadzu, Kyoto, Japan). A  
129 Phenomenex Luna Omega C18 column (100 × 2.1 mm, 1.6 µm particle size, Phenomenex,  
130 Aschaffenburg, Germany) was employed for the analysis of extracts, fractions, and pure  
131 compounds during isolation and method development. Quantification of mogroside V (**3**) was  
132 performed on a Nucleodur C18 Pyramid (250 × 4.6 mm, 5 µm, Macherey-Nagel, Düren,  
133 Germany) by triplicate injections of both, the mogroside reference and the luohanguo sample.

134

### 135 2.3. NMR spectroscopy

136

137 NMR spectra were recorded using a Bruker Avance III 400 NMR spectrometer (Bruker  
138 Biospin, Rheinstetten, Germany) operating at 400.33 MHz for the proton channel and at 100.66  
139 MHz for the  $^{13}\text{C}$  channel by means of a 5 mm PABBO broad-band probe with a  $z$  gradient unit.  
140 Measurements were performed at 293 K; the temperature in the probe head was calibrated with  
141 a methanol- $d_4$  solution and regulated within 0.1 K during the measurements. For each sample,  
142 automatic tuning and matching of the probe was performed, as was automatic shimming of the  
143 on-axis shims ( $z$  to  $z^5$ ). The automatic receiver gain adjustment mode afforded the maximum  
144 gain value in all measurements. Bruker Topspin software 3.6.0 was employed for spectra  
145 recording.

146 Characterization of the purified sample in pyridine- $d_5$  and DMSO- $d_6$  was accomplished by  
147 use of conventional full spectral range routine parameters and pulse programs for structure  
148 elucidation.

149

#### 150 2.3.1 Quantitative $H,H$ COSY measurements

151

152 The non-phase-sensitive pulse program *cosygpmfzf* (with gradient pulses) and double  
153 quantum filter selection via the gradient ratio supplied by the manufacturer were used for  
154 correlated spectroscopy (COSY) measurements. Spectral width was set to  $3.10 \pm 2.40$  ppm (a  
155 range of 1921 Hz) in both dimensions, with 1024 data points being collected in F2 and 128  
156 increments in the indirect (F1) dimension. Acquisition time was calculated to be 0.267 s, and  
157 the interscan-delay was 3 s. With two scans collected per increment and 16 dummy scans, the  
158 total measuring time amounted to 14 min and 50 s ('2-scan-COSY'); with eight scans, about 57  
159 minutes were required to record the spectrum ('8-scan-COSY').

160 The raw data were processed as follows: zero filling to an  $8k \times 8k$  matrix, then  
161 multiplication with a sine function before two-dimensional Fourier transformation and  
162 magnitude calculation in F2, with automatic baseline correction in both dimensions and  
163 symmetrization of the resulting spectrum. Integration borders were set uniformly by using the  
164 same integration file with a range of 3.762 to 3.604 ppm for F2 and 1.792 to 1.612 ppm in F1.

165

### 166 2.3.2. Quantitative band-selective $^1\text{H}$ , $^{13}\text{C}$ HSQC measurements

167

168 Band-selective heteronuclear single quantum correlation spectroscopy (bs-HSQC)  
169 measurements for quantification were performed using the phase-sensitive *shsqctgpsi2.2* pulse  
170 program of the Bruker pulse program library with a band-selective shaped  $^{13}\text{C}$  refocusing pulse  
171 and  $^{13}\text{C}$  GARP decoupling. The  $^1\text{H}$  spectral range was  $(4.50 \pm 5.05)$  ppm, spectral range 4006  
172 Hz, whereas the  $^{13}\text{C}$  spectral range was  $(77.2 \pm 5.0)$  ppm, corresponding to 1006 Hz.

173 The shape form Q3.1000 was chosen for the selective refocusing pulse and, in order to  
174 achieve selective excitation over the frequency range of 1000 Hz (10 ppm), the length of the  
175 pulse was determined to 3448  $\mu\text{s}$  with a power of 0.0986 W for the probe head in use. For the  
176  $^1\text{H}$  channel, 1024 data points were collected, whereas for the  $^{13}\text{C}$  channel, 64 data points were  
177 set. The acquisition time was 0.128 s, and the inter-scan delay was set to 3.15 s. The relevant  
178 delays in the pulse program were set corresponding to a coupling constant of  $^1J_{\text{CH}} = 135$  Hz.  
179 With 16 dummy scans and 16 scans per increment, the total acquisition time for this HSQC  
180 experiment was about 57 minutes.

181 The raw data were processed as follows: zero filling to a  $4k \times 4k$  matrix and then  
182 multiplication of both dimensions with a squared sine function before two-dimensional Fourier  
183 transformation and phase correction. Phase correction parameters of the previous experiment  
184 were used and were carefully visually controlled and manually adopted for the relevant cross  
185 peak in both dimensions for each measurement. After automatic baseline correction in both



186 dimensions, integration borders were set uniformly by using the same integration file with a  
187 range of 3.77 to 3.60 ppm in F2 ( $^1\text{H}$ ) and 78.10 to 76.26 ppm in F1 ( $^{13}\text{C}$ , bs-HSQC<sub>wide</sub>).  
188 Additionally, an alternate integration range (bs-HSQC<sub>small</sub>) was used with much narrower  
189 ranges of 3.77 to 3.60 ppm in F2 ( $^1\text{H}$ ) and 77.37 to 76.76 ppm in F1 ( $^{13}\text{C}$ ).

190

#### 191 2.4. Extraction and isolation

192

193 A total of 600 g powdered dried fruits was exhaustively extracted with methanol by  
194 maceration, and the solvent was evaporated under reduced pressure to yield 114.3 g crude  
195 extract. The crude extract was dissolved in 300 mL water and chromatographed over Diaion  
196 HP-20, with subsequently elution with water, methanol 30%, methanol 80%, and methanol  
197 100%. The methanol 80% fraction (17.5 g) was subjected to silica gel column chromatography  
198 by using dichloromethane–methanol–water in three portions of 815 mL with the following  
199 ratios: 8:2:0.2, 7:3:0.5, and 6:4:1. Of the resulting eight fractions (A–H), fraction G (8.70 g)  
200 was chromatographed with Sephadex LH-20 to give another five fractions (G1–G5). Fraction  
201 G3 (5.70 g) was subjected to preparative MPLC by applying a solvent mixture of 0.1% formic  
202 acid in water (solvent A) and methanol (solvent B) with the following gradient: 38% B to 45%  
203 B in 60 min, and to 95% B in 30 min. Of the resulting five fractions (G3A–G3E), fraction G3B  
204 (716 mg) was chromatographed using silica gel flash chromatography and a gradient of  
205 dichloromethane–methanol–water (8:2:0.2 to 7:3:0.5) to give six fractions. The third fraction  
206 (211 mg) was separated by semi-preparative HPLC by using 0.025% formic acid in water  
207 (solvent A) and acetonitrile (solvent B) with a gradient of 25% B to 30% B in 30 minutes, a  
208 flow rate of 2 mL/min, and an oven temperature of 35°C, to give 26.9 mg compound **1** and 27.5  
209 mg compound **3**. Fraction G3C (371 mg) was purified using normal phase solid phase extraction  
210 to give another 113.8 mg compound **3**. Fraction G3D (242 mg) was subjected to semi-

211 preparative HPLC by using 0.025% formic acid in water (solvent A) and acetonitrile (solvent  
212 B) with a gradient of 20% B to 25% B in 30 minutes, a flow rate of 3 mL/min, and an oven  
213 temperature of 35°C, to give 27.5 mg compound **2** and 32.3 mg compound **4**.

214

#### 215 *2.5. Quantitative analysis*

216

217 A total of 1.00 g dried and ground fruits was extracted three times with 50 mL methanol-  
218 water 80% (v/v) by using ultra-sonication for 15 min each. After filtration, the solution was  
219 evaporated to dryness. The residue was re-dissolved in 3 mL methanol-water 20% (v/v) and  
220 subjected to an equilibrated SPE C-18 column (1 g, 6 mL). After the column had been washed  
221 with three column volumes of methanol-water 20% (v/v), the desired compounds were eluted  
222 with three column volumes of methanol (100%). The combined methanol fractions were  
223 evaporated to dryness, re-dissolved in 600  $\mu$ L DMSO- $d_6$ , and transferred to NMR sample tubes.  
224 For calibration, 26.4 mg mogroside V (**3**) were dissolved in 1000  $\mu$ L DMSO- $d_6$  and diluted to  
225 the desired concentrations with the same solvent. Purity of the compound was assessed using  
226 1,2,4,5-tetrachloro-3-nitrobenzene (6.20 mg) as the internal standard.

227 For the quantification of 11- $\alpha$ -hydroxy-mogrosides, calibration solutions 1–5 with  
228 concentrations of 20.34, 15.26, 8.48, 3.39, and 1.70 mmol/L were prepared and analyzed with  
229 bs-HSQC and H,H COSY measurements. For the latter experiment, two different parameter  
230 sets were investigated by using either 2 or 8 scans and the resulting acquisition times of 15 min  
231 or 57 min, respectively.

232

#### 233 *2.6. Method validation*

234

235 The developed method was validated for linearity, repeatability, precision, accuracy, and  
236 limit of quantification. Evaluation of linearity was achieved by establishing calibration curves  
237 over a range of at least 80 to 120% of the measured concentrations. Therefore, 5-point  
238 calibration curves were created and expressed as linear functions. In order to define a limit of  
239 quantitation, a solution of 1.00 mmol/L mogroside V (**3**) was prepared. Precision and  
240 repeatability were assessed using samples of luo han guo. Repeatability measurements were  
241 conducted six times on the same sample. For the determination of precision, six different  
242 samples were prepared and measured once within one day (intra-day precision) or on two  
243 different days (inter-day precision). Determination of accuracy was accomplished by spiking  
244 the samples with various amounts of standard solution as follows:

- 245
- 246 - high spike (120%): 150  $\mu$ L sample + 450  $\mu$ L calibration solution 2
  - 247 - medium spike (100%): 150  $\mu$ L sample + 225  $\mu$ L calibration solution 2  
248 + 225  $\mu$ L calibration solution 3
  - 249 - low spike (80%): 150  $\mu$ L sample + 450  $\mu$ L calibration solution 3
- 250

251 All obtained values were expressed as % recovery by using the mean value of the inter-day  
252 measurements (N=12) for the sample concentration. Additionally, an overall mean value was  
253 calculated from the inter-day measurements of all four experimental results (N=48), and the  
254 deviations of the results obtained from the four methods were compared.

255

### 256 **3. Results and discussion**

257

#### 258 *3.1. Isolation of standard compounds and revision of NMR data*

259

260 As a first step, standard compounds were isolated for method development and eventual  
261 validation. At least one compound with an  $\alpha$ -hydroxy-group in position C-11 and one  
262 compound without this structural feature were required. Therefore, we focused on the isolation  
263 of mogroside V (**3**) and 11-oxo-mogroside V (**1**), the two most abundant mogrosides in the ripe  
264 fruits of *S. grosvenorii* (Shen et al., 2014). The isolation steps followed in principle the  
265 procedure described by Li et al. (2006) for the isolation of mogroside V (**3**). The isolation  
266 process was monitored by LC-DAD-ELSD and LC-MS using the method described by Qing et  
267 al. (2017).

268 All in all, four cucurbitane glycosides were obtained and identified as 11-oxo-mogroside V  
269 (**1**), mogroside IVe (**2**), mogroside V (**3**), and 11-deoxymogroside V (**4**) by using MS and NMR  
270 experiments and comparisons with literature data (Akihisa et al., 2007; Chaturvedula, &  
271 Prakash, 2011; Kasai et al., 1989; Niu et al., 2017; Prakash, & Chaturvedula, 2014; Qing et al.,  
272 2017). However, the reported NMR shift values for mogroside V (**3**) and 11-oxo-mogroside V  
273 (**1**) (Chaturvedula, & Prakash, 2011) differed significantly from our own NMR measurements  
274 and from the NMR data of similar compounds (Akihisa et al., 2007; Niu et al., 2017). Revised  
275 NMR data for the two major components mogroside V (**3**) and 11-oxo-mogroside V (**1**) are  
276 given in Tables S1 and S2 together with those of the other two isolated compounds. Moreover,  
277 we reassigned shift values for five signals of mogroside IVe (**2**), which had not been  
278 unambiguously assigned by the time of its structure elucidation (Kasai et al., 1989).  
279 Additionally, we added missing values for the sugar moieties of the compound also referred to  
280 as mogroside IV in older references. The NMR spectra of all four compounds are depicted in  
281 Figs. S1–S30.

282

283 *3.2. Method development*

284

### 285 3.2.1. Selection of NMR solvents and signals for quantification

286

287 In our quest to identify and quantify all 11- $\alpha$ -hydroxy-mogrosides, we first analyzed  
288 significant signals of the terpenoid moiety by comparing mogroside V (**3**) and 11-oxo-  
289 mogroside V (**1**). Several prerequisites had to be fulfilled for the selective quantification of the  
290 11- $\alpha$ -hydroxylated species, in addition to structures with either a methylene group or a carbonyl  
291 function in the respective position (see Fig. 1). Because of the severe overlap of many aliphatic  
292 signals of the terpenoid ring system, the high frequency shifted methine proton next to the  
293 hydroxyl group (H-11) displays a unique feature of sweet-tasting mogrosides. In the one-  
294 dimensional  $^1\text{H}$  NMR spectrum recorded in pyridine- $d_5$ , this signal unfortunately overlapped  
295 several methine signals of the glucose moiety. Thus, direct integration was not possible. HSQC  
296 experiments showed similar results, because the shift value of C-11 was also within the bulk of  
297 glucose signals. However, selectivity was achieved when the nuclei in the neighbourhood of  
298 this proton were considered. H-11 showed coupling with the two protons in position 12, both  
299 having a chemical shift of 2.19 ppm (Table S2). This coupling appeared as a clearly separated  
300 cross peak in the two-dimensional H,H COSY spectrum for the 11- $\alpha$ -hydroxy-mogrosides and  
301 showed no overlap with any sugar signals (Fig. S15, 4.18 ppm/2.19 ppm).

302 NMR spectra for compounds **1** and **3** were additionally recorded in DMSO- $d_6$ , because of its  
303 potent solvency for both terpene glycosides and the crude extracts. Moreover, dimethyl  
304 sulfoxide is a far more economic NMR solvent. Again, 1D proton NMR spectra did not provide  
305 sufficient resolution for the H-11 methine signal (Fig. S19), which now overlapped with three  
306 other diastereotopic protons of the terminal glucose methylene groups GII, GIV, and GV (Fig.  
307 1). However, this time not only H,H COSY measurements showed good resolution (Fig. S21),  
308 but also HSQC experiments clearly separated the CH-11 cross peak from all other glucose  
309 signals (Fig. S22). Consequently, DMSO- $d_6$  was chosen as the NMR solvent, and the cross

310 peak of the CH-11 correlation at 3.67 ppm/76.7 ppm (HSQC) and the cross coupling of the H-  
311 11 methine signal with the H-12 methylene protons at 3.67 ppm/1.67 ppm (H,H COSY) were  
312 selected for further method development.

313

### 314 3.2.2. Extraction and sample preparation

315

316 For the extraction of the dried fruits, pure methanol (Shen et al., 2014) or methanol-water  
317 (80% v/v) (Qing et al., 2017) have been described as suitable solvents for analytical purposes,  
318 with a ratio of 1 g powdered plant material to 100 mL of solvent being applied. In our study,  
319 the use of methanol resulted in a yield of approximately 24% (w/w) of crude extract calculated  
320 based on the amount of dried fruits, whereas the methanol-water mixture delivered 36% (w/w)  
321 of crude extract. The higher mass fraction of the methanol-water extract was expected, and a  
322 higher concentration of  $\alpha$ -hydroxy-mogrosides was observed. LC-MS analysis of the crude  
323 extracts revealed that both solvents efficiently extracted mogrosides with two, three, four, or  
324 five sugar moieties, but only the methanol-water mixture yielded hexaglycosidic mogrosides.  
325 Thus, methanol-water 80% (v/v) was used for subsequent extractions.

326 In order to increase the concentration of  $\alpha$ -hydroxy-mogrosides and to reduce NMR  
327 measurement time, the crude extract was further purified by C-18 solid phase extraction.  
328 Therefore, various methanol-water mixtures (0, 20, 50, and 80%) were evaluated for their  
329 ability to wash polar analytes off the column without eluting the compounds of interest. LC-  
330 MS analysis confirmed that, with methanol (20%), a large number of unwanted constituents  
331 were removed before elution of the  $\alpha$ -hydroxy-mogrosides with pure methanol. This procedure  
332 significantly increased the concentration of the  $\alpha$ -hydroxy-mogrosides, leading to intense  
333 signals in both the H,H COSY and HSQC experiments.

334

### 335 3.2.3. Homonuclear two-dimensional NMR (H,H COSY)

336

337 Utilizing the standard pulse programs delivered by the spectrometer manufacturer, we  
338 developed a method for the measurement and integration of several H,H COSY spectra. H,H  
339 COSY measurements provide the option of the selective detection of one special coupling via  
340 the corresponding cross peak with proton excitation and proton detection at 3.67 ppm/1.67 ppm.  
341 Among several H,H COSY variants, double quantum filtered experiments involving the  
342 application of gradient pulses and thereby the suppression of singlets and artefacts are  
343 considered extremely robust (Shaw, Salaun, Dauphin, & Ancian, 1996). We employed an  
344 established simple non-phase-sensitive measurement allowing easy integration of parts of the  
345 2D plot. Because only one signal region was of interest, we used a small spectral width,  
346 observing the aliphatic region in the range of 0.7 to 5.5 ppm and thus reducing measurement  
347 time (Fig. 2). The crucial experimental parameter to be investigated for quantitative analysis is  
348 the scan repetition time, as this parameter is responsible for the length of the NMR experiment.  
349 It has to be sufficiently long to allow complete relaxation of the protons. We investigated this  
350 parameter by running H,H COSY experiments with various delays between 0.5 and 20 s for the  
351 standard compound (**3**) and the extract after sample preparation. No significant differences of  
352 the integrals of the cross peak of H-11/H-12 in the two cases were observed in the scan  
353 repetition time range of 2 s to 20 s (data not shown). Thus, a setting of 3 s was used for all H,H  
354 COSY experiments in this study. Two measurements were made: a fast 2-scan-COSY (15 min)  
355 and an 8-scan-COSY (57 min) with improved signal to noise ratio. During the evaluation of the  
356 processing and integration parameters, we obtained most reproducible results by improving the  
357 resolution by zero filling and, after automatic baseline correction on both dimensions, by  
358 symmetrizing the H,H COSY spectrum (see section 2.3.1.).

359

#### 360 3.2.4. Heteronuclear two-dimensional NMR (HSQC)

361

362 The other nucleus in the neighbourhood of the H-11 methine proton is the carbon atom at  
363 position 11. This one-bond coupling is responsible for the cross signal in the HSQC spectrum  
364 at 3.67 ppm/76.7 ppm (Fig. 3). Here, protons are excited, the polarization is transferred to the  
365 carbon atom and back to the proton again, which are then detected in a sensitive manner  
366 (Schleucher et al., 1994). We used this approach as a second quantitative method and observed  
367 that no actual overlap occurs with any glucose signals. For the optimization of this HSQC  
368 experiment, we investigated once more the effect of the relaxation time and found no significant  
369 difference between delays of 2 to 20 s (data not shown). Therefore, a value of about 3 s was  
370 also chosen for this experiment. We drastically reduced the number of increments for the carbon  
371 frequency by working with band-selective excitation of only a range of 10 ppm (Girreser,  
372 Ugolini, & Çiçek, 2019). Furthermore, delays in the pulse program were adapted to the coupling  
373 constant of this methine unit (Çiçek, Ugolini, & Girreser, 2019), which we determined at 135  
374 Hz. Finally, we compared the traditional recording of each increment with non-uniform  
375 sampling (Jaravine, Ibraghimov, & Orekhov, 2006) and obtained more reproducible results  
376 with traditional sampling (data not shown). In this manner, we created a method requiring a  
377 measuring time of about 57 min. Again, we paid attention to the data processing by zero filling  
378 of the 2D matrix, automatic baseline correction, and the selection of a proper integration range.  
379 In this case, we selected a small and a wide integration range and compared the results of the  
380 different ranges (see section 2.3.2).

381

#### 382 3.3. Method validation

383

##### 384 3.3.1. Linearity and quantitation limit



385

386 For the validation of linearity, calibration curves in four different modes were established  
387 over a concentration range of 1.70 to 20.34 mmol/L, with mogroside V (**3**) as an external  
388 calibration standard (Table 1). Purity of the compound was checked by using a certified  
389 reference standard (1,2,4,5-tetrachloro-3-nitrobenzene) and integration of the H-6 in the  
390 cucurbitane scaffold, plus the H-6b of the G<sub>I</sub> glucose moiety, by 1D proton NMR. The purity  
391 of mogroside V (**3**) was determined to be 99.09%.

392 All four calibration curves showed acceptable coefficients of determination, with values  
393 between 0.9965 and 0.9986 (Table 1). In the HSQC experiments, both modes of integration  
394 yielded almost the same slopes and only differed in their offsets, which were naturally higher  
395 for the wide integration range. The differences between the two COSY experiments were  
396 characterized by a significantly higher slope for the 8-scan-COSY, which furthermore showed  
397 a negligible offset.

398 Because of the use of integration fields instead of the threshold integration, a limit of  
399 quantitation had to be defined. Therefore, a solution of 1.00 mmol/L was prepared and  
400 determined under the four measurement/integration modes. Whereas, with the 8-scan-COSY,  
401 this concentration was determined within 50% of the actual value, the other three modes did  
402 not show sufficient accuracy at this level. For these three modes, the limit of quantitation was  
403 defined as 1.70 mmol/L (Table 1). When these values were calculated as mogroside V (**3**), as  
404 we did in the quantitative assays (Table 2), they corresponded to 1.3 mg/mL (1.00 mM) or 2.2  
405 mg/mL (1.70 mM), respectively. Because 1.00 g luo han guo was applied in the assays, the  
406 same concentrations are present per gram of dried fruit.

407

408 3.3.2. Precision and repeatability

409

410 HSQC measurements showed similar repeatability, with a relative standard deviation of  
411 3.38% for the wide integration mode and 3.25% for the small integration parameters (Table 2).  
412 Moreover, in terms of precision, both variants were comparable, with RSD values between  
413 5.45% and 6.35%. H,H COSY measurements showed better repeatability than the HSQC  
414 experiment, with RSD values of 1.95% for the 2-scan-COSY and 1.89% for the 8-scan-  
415 experiment. The latter experiment additionally displayed excellent values during the precision  
416 measurements, with relative standard deviations of 1.66 to 1.73%. The 2-scan COSY, in  
417 contrast, showed RSD values similar to those of the HSQC experiment, with relative standard  
418 deviations of 4.43 to 5.37%. Interestingly, no significant differences were observed between  
419 the intra-day and inter-day measurements, indicating the robustness of the developed NMR  
420 methods (Table 2).

421

### 422 3.3.3. Accuracy and comparability

423

424 Spiking experiments were conducted for the determination of accuracy (Table 3). Various  
425 calibration solutions were used to achieve concentrations of 80, 100, and 120% of the assay  
426 concentration (mean values of the precision measurements). With regard to the HSQC  
427 experiments, both integration methods revealed good recovery rates and showed slightly better  
428 recoveries for the small integration range. H,H COSY measurements also resulted in excellent  
429 recovery rates, with maximum deviations of 4.9% for the 2-scan-experiment and 2.8% for the  
430 8-scan-COSY. In addition, the mean values obtained from the precision measurements were  
431 compared with each other and showed usual deviations of not more than 3% (Table 3).

432

### 433 3.3.4. Specificity and selectivity

434

435 The total content of 11- $\alpha$ -hydroxy-mogrosides can be determined from both the HSQC  
436 experiment and the H,H COSY measurements. Moreover, these value-determining compounds  
437 can be quantified among additional non-sweet-tasting derivatives, e.g., 11-oxo-mogrosides or  
438 11-deoxy-mogrosides. Therefore, the present methods can be rendered specific and selective at  
439 the same time. The selective determination of the sweetening principle can be achieved in two  
440 ways: either by direct observation of the CH-11 methine unit (HSQC) or, alternatively, through  
441 indirect (H,H COSY) measurement via the coupling to the methylene group in the  
442 neighbourhood (CH<sub>2</sub>-12). This highlights the advantage of NMR spectroscopy over other  
443 analytical methods, namely its characteristic measuring principle and the possibility of  
444 quantifying the structural features necessary for the biological effect.

445

#### 446 3.4. Quality control

447

448 In the above, we have presented two experiments for the quality control of *S. grosvenorii*.  
449 The amount obtained for the 11- $\alpha$ -hydroxy-mogrosides was determined as being 15.2 to 16.2  
450 mg/g dried fruit (calculated as mogroside V). In comparison, the amount of mogroside V (**3**)  
451 was determined as 9.2 mg/g dried fruit by using the method of the Food Chemicals Codex (Figs.  
452 S31 and S32) (FCC 11, 2018). This value is in accordance with the average amounts described  
453 in the literature for mogroside V (**3**), namely 9.5 mg/g (Li et al., 2014) or 10.5 mg/g (Pawar et  
454 al., 2013), respectively. However, the significantly lower value compared with our assays  
455 indicates the large amounts of additional constituents that contribute to the sweetening effect  
456 of luo han guo and that are not quantified with the chromatographic methods reported to date.

457 We investigated two variants in the two experiments. For the HSQC measurements, we used  
458 different integration ranges (bs-HSQC<sub>wide</sub> and bs-HSQC<sub>small</sub>), whereas for the H,H COSY  
459 experiments different scan numbers were applied (2-scan-COSY and 8-scan-COSY). For the

460 HSQC experiment, a selective pulse program decreased the  $^{13}\text{C}$  spectral range to 10 ppm and  
461 thus significantly reduced the measurement time. Validation of the four resulting methods  
462 according to the ICH guideline Q 2 R(1) have revealed similar values for the two HSQC variants  
463 thus indicating the applicability of the two integration methods. For the H,H COSY  
464 measurements, a 2-scan experiment was investigated for the fast quantification (15 min) of 11-  
465  $\alpha$ -hydroxy-mogrosides, in addition to an 8-scan variant, resulting in the same measurement time  
466 as in the HSQC experiments (57 min). The 2-scan-COSY revealed similar validation results as  
467 the HSQC experiments, whereas the 8-scan-COSY was superior in terms of accuracy, precision,  
468 and limit of quantitation.

469 Furthermore, all methods were able selectively to quantify the total content of the value-  
470 determining 11- $\alpha$ -hydroxy-mogrosides. Because the assay is based on molarity (and the content  
471 is subsequently referenced to mogroside V), the method can also be applied to unripe fruits,  
472 and the sweetening potential can be predicted and estimated at an early stage of cultivation.  
473 Another issue when dealing with luohan guo is the possible dilution of extracts with extracts  
474 of unripe fruits (Pawar et al., 2013). Although not being intended for the detection of  
475 adulterations, our method can also be performed to address this problem by using the cross  
476 correlations of the H-6 protons of the non-terminal glucose moieties  $G_I$  and  $G_{III}$  (Fig. 1). These  
477 cross peaks can be found in the H,H COSY spectrum at 3.57/3.90 ppm for  $G_I$  and at 3.40/4.11  
478 ppm for  $G_{III}$  and have a ratio of 2:1 with regard to the H-11/H-12 cross peak of pure mogroside  
479 V (**3**) (Fig. 2). In luohan guo samples, this ratio is approximately 2.75:1. The higher ratio results  
480 from the remaining mogrosides, which obviously show similar grades of glycosylation.  
481 However, in the case of dilution with unripe fruits, the ratio would be far below 2:1, because of  
482 the increased presence of mogrosides with only two terminal sugar moieties (one at C-3 and  
483 one at C-24) (Itkin et al., 2016). Thus, the characteristic signals of the non-terminal glucose  
484 moieties would be significantly reduced (or absent in the case of complete falsification). The

485 detection of adulteration would also be feasible with the HSQC experiment by using the  
486 respective C-H correlations. Here, a ratio of 0.6:1 was observed in our experiments for  
487 mogroside V (**3**) and 0.85:1 for luohan guo samples. However, in the band-selective mode, the  
488  $^{13}\text{C}$  spectral width would have to be increased resulting in longer measurement times.

489 Analysis time is an important issue when dealing with quality control methods and is one  
490 of the reasons that two-dimensional NMR methods are readily overlooked. However, in the  
491 present study and with regard to the application of band-selective approaches for the HSQC  
492 experiment, we have demonstrated that even heteronuclear techniques deliver precise and  
493 accurate results within reasonable measurement times. For example, in the HPLC assay for the  
494 mogroside V (**3**) content of the Food Chemicals Codex, the last peak in the extract eluted after  
495 more than 50 minutes (Fig. S32). Thus, a measurement time of 60 minutes was chosen, which  
496 corresponds to the measurement times of three of our methods. Chromatographic separation of  
497 extracts will always need several minutes of elution time, especially for more complex extracts  
498 such as the extracts of luohan guo. Elution times can (to some extent) be decreased using  
499 smaller particle sizes, selective extraction, or mass spectrometric detection methods. Deng et  
500 al. (2013) have used micelle-mediated cloud-point extraction and quantified mogroside V (**3**)  
501 in 20 minutes. However, the relatively low accuracy and precision values and the extraction  
502 yield of only 80% in their investigation are major shortcomings for the quality control of luohan  
503 guo. In two other studies, LC-MS was applied in the multiple reaction monitoring (MRM)  
504 mode and quantified five and eight mogrosides, respectively (Shen et al., 2014; Luo et al.,  
505 2016). The analysis time of the two methods was 12 and 10 minutes and thus in the range of  
506 the 2-scan-COSY experiment. Moreover, in terms of accuracy and precision, the two LC-MS  
507 methods are comparable with the 2-scan-COSY, showing slightly better precision values and  
508 somewhat lower recovery rates. The linear range of MRM methods usually is in the nanomolar  
509 scale and obviously results in lower limits of quantification. These low LoQs render MRM

510 methods an ideal tool for trace analysis. For quality control assays, however, the LoQ is not a  
511 crucial parameter and is not even requested in the respective ICH guideline, because the assay  
512 concentration is determined during method development. Nevertheless, broader quantitation  
513 ranges paired with selectivity allow easier method adaption to other purposes, e.g., analysis of  
514 dietary supplements. Both characteristics are given for the NMR methods described herein. In  
515 contrast to all previously reported assays, all (rather than just a few) of the sweet-tasting 11- $\alpha$ -  
516 hydroxy-mogrosides have been quantified in the ripe fruits of *Siraitia grosvenorii*.

517

#### 518 **4. Conclusion**

519

520 In this study, two-dimensional quantitative NMR was successfully applied for the analysis  
521 of *S. grosvenorii* fruits. The determination of the total content of sweet-tasting mogrosides was  
522 accomplished by using NMR signals resulting from the 11- $\alpha$ -hydroxy-group that occurs in this  
523 particular compound class and that is the crucial structural feature for the sweetening effect. In  
524 contrast to our previous work in which we quantified the total amount of a compound class by  
525 one specific NMR signal (Çiçek, Girreser, & Zidorn, 2018), only the compounds relevant for  
526 the biological effect were determined this time. The selective quantification of bioactive  
527 compound (sub)classes is not only a valuable tool for the quality control of food ingredients or  
528 herbal medicines but can also be applied to the screening of extracts during, for example, drug  
529 discovery. Furthermore, the present study provides another example for the advantage of  
530 quantitative NMR spectroscopy in natural products analysis in which several constituents  
531 contribute to a biological effect.

532

#### 533 **Funding**

534

535 This research received no specific grant from funding agencies in the public, commercial,  
536 or not-for-profit sectors.

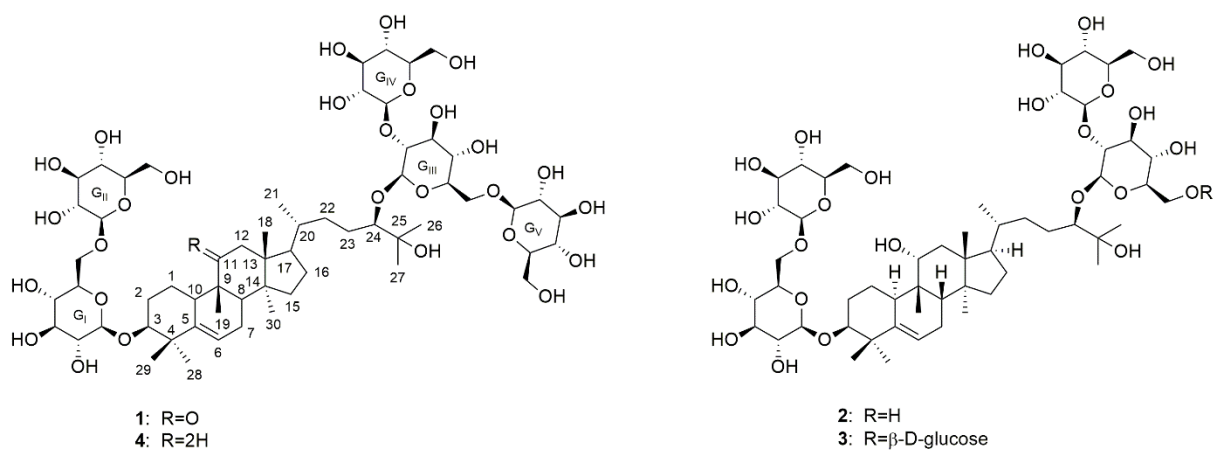
537

538

accepted manuscript

539 **Figures**

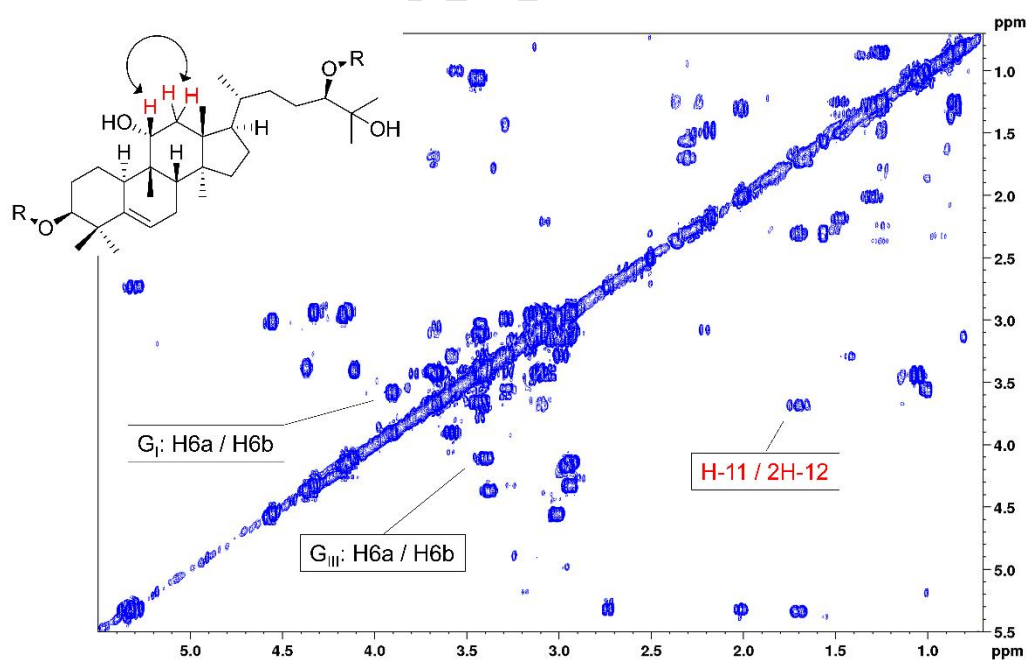
540



541

542 Fig. 1: Chemical structures of 11-oxomogroside V (1), mogroside IVe (2), mogroside V (3),  
543 and 11-deoxymogroside V (4). Exact stereochemistry can be retrieved from compounds 2 and  
544 3.

545

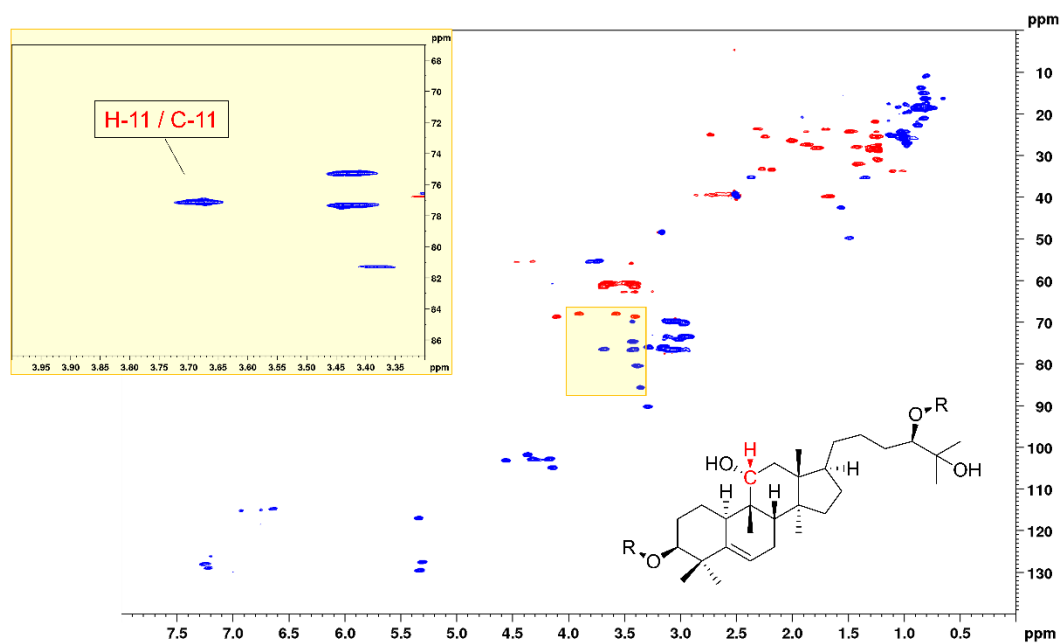


546

547 Fig. 2: H,H COSY diagram of luohan guo sample recorded in DMSO-*d*<sub>6</sub> in the region of 0.7 to  
548 5.5 ppm. The signal used for quantitative NMR is highlighted in red.

549





550

551 Fig. 3: Complete spectral range HSQC diagram of luohan guo sample recorded in DMSO-*d*<sub>6</sub>  
 552 and band-selective HSQC diagram in the region of 3.3 to 4.0 ppm (<sup>1</sup>H) and 67 to 87 ppm (<sup>13</sup>C)  
 553 (top left, only signals in the <sup>13</sup>C-range from 72.2 to 82.2 ppm are detected). Signal used for  
 554 quantitative NMR is highlighted in red.

555

556

557

558 **Table 1**  
 559 Regression equations, coefficients of determination ( $R^2$ ), and limits of quantitation (LoQ)  
 560 obtained from various NMR measurements (y: 2D NMR integral in arbitrary units, x:  
 561 concentration in mmol/L)

Measurement	Regression equation	$R^2$	LoQ
bs-HSQC (wide integration)	$y = 44.04 \times 10^6 x + 11.78 \times 10^6$	0.9965	1.70 mM
bs-HSQC (small integration)	$y = 45.86 \times 10^6 x - 20.80 \times 10^6$	0.9981	1.70 mM
H,H COSY (2 scans, 15 min)	$y = 40.58 \times 10^6 x - 59.16 \times 10^6$	0.9970	1.70 mM
H,H COSY (8 scans, 57 min)	$y = 174.67 \times 10^6 x - 6.60 \times 10^6$	0.9986	1.00 mM

562  
 563  
 564  
 565  
 566  
 567  
 568  
 569  
 570  
 571

**Table 2**  
 Repeatability and intra-day and inter-day precision obtained from various NMR  
 measurements. Results are given in mg/g drug material; RSD values are shown in parenthesis.

Measurement	Repeatability	Intra-day 1	Intra-day 2	Inter-day
bs-HSQC <sub>wide</sub>	15.57 (3.38%)	16.21 (6.35%)	16.13 (5.45%)	16.17 (5.65%)
bs-HSQC <sub>small</sub>	15.55 (3.25%)	15.87 (5.73%)	16.02 (6.00%)	15.95 (5.61%)
H,H COSY <sub>2 scans</sub>	14.94 (1.95%)	15.00 (5.10%)	15.85 (4.43%)	15.43 (5.37%)
H,H COSY <sub>8 scans</sub>	14.98 (1.89%)	15.20 (1.73%)	15.28 (1.71%)	15.24 (1.66%)

572  
 573  
 574  
 575  
 576  
 577  
 578  
 579  
 580  
 581  
 582

**Table 3**  
 Accuracy of various NMR measurements. Values are expressed as the percentage of recovery  
 (spiking experiments) and deviation from the mean value of all four experimental variants.

Measurement	High spike (120%)	Medium spike (100%)	Low spike (80%)	Deviation from the mean value
bs-HSQC <sub>wide</sub>	101.2%	94.1%	89.3%	+3.0%
bs-HSQC <sub>small</sub>	95.2%	96.2%	93.8%	+1.6%
H,H COSY <sub>2 scans</sub>	95.1%	103.2%	97.6%	-1.7%
H,H COSY <sub>8 scans</sub>	97.2%	98.8%	101.3%	-2.9%

583

584 **References**

- 585 Akihisa, T., Hayakawa, Y., Tokuda, H., Banno, N., Shimizu, N., Suzuki, T., & Kimura, N.  
586 (2007). Cucurbitane glycosides from the fruits of *Siraitia grosvenorii* and their inhibitory  
587 effects on Epstein-Barr virus activation. *Journal of Natural Products*, 70, 783–788.  
588 <https://doi.org/10.1021.np068074x>.
- 589 Chaturvedula, V. S. P., & Prakash, I. (2011). Cucurbitane glycosides from *Siraitia grosvenorii*.  
590 *Journal of Carbohydrate Chemistry*, 30, 16–26.  
591 <https://doi.org/10.1080/07328303.2011.583511>.
- 592 Çiçek, S. S., Girreser, U., & Zidorn, C. (2018). Quantification of the total amount of black  
593 cohosh cycloartanoids by integration of one specific <sup>1</sup>H NMR signal. *Journal of*  
594 *Pharmaceutical and Biomedical Analysis*, 155, 109–115.  
595 <https://doi.org/10.1016/j.jpba.2018.03.056>.
- 596 Çiçek, S. S., Ugolini, T., & Girreser, U. (2019). Two-dimensional qNMR of anthraquinones in  
597 *Frangula alnus* (*Rhamnus frangula*) using surrogate standards and delay time adaption.  
598 *Analytica Chimica Acta*, 1081, 131–137. <https://doi.org/10.1016/j.aca.2019.06.046>.
- 599 Çiçek, S. S. (2020). Structure-dependent activity of plant-derived sweeteners. *Molecules*, 25,  
600 1946. <https://doi.org/10.3390/molecules25081946>.
- 601 Deng, F. L., Liang, X. F., Yang, L. R., Liu, Q. F., & Liu, H. Z. (2013). Analysis of mogroside  
602 V in *Siraitia grosvenorii* with micelle-mediated cloud-point extraction. *Phytochemical*  
603 *Analysis*, 24, 381–385. <https://doi.org/10.1002/pca.2420>.
- 604 Fletcher, J. N., Pan, L., & Kinghorn, A.D. (2017). Medicinal chemistry of plant naturals as  
605 agonists/antagonists for taste receptors. In: D. Krautwurst, D. (Ed.), *Taste and Smell;*  
606 *Topics in Medicinal Chemistry* (pp. 35–72). Heidelberg: Springer.
- 607 Girreser, U., Ugolini, T., & Çiçek, S. S. (2019). Quality control of *Aloe vera* (*Aloe barbadensis*)  
608 and *Aloe ferox* using band-selective quantitative heteronuclear single quantum correlation

609 spectroscopy (bs-qHSQC). *Talanta*, 205, 120109.  
610 <https://doi.org/10.1016/j.talanta.2019.07.004>.

611 Gong, X., Chen, N., Ren, K., Jia, J., Wei, K., Zhang, L., Lv, Y., Wang, J., & Li, M. (2019). The  
612 fruits of *Siraitia grosvenorii*: A review of a Chinese food-medicine. *Frontiers in*  
613 *Pharmacology*, 10, 1400. <https://doi.org/10.3389/fphar.2019.01400>.

614 Itkin, M., Davidovich-Rikanati, R., Cohen, S., Portnoy, V., Doron-Faigenboim, A., Oren, E.,  
615 Freilich, S., Tzuri, G., Baranes, N., Shen, S., Petreikov, M., Sertchook, R., Ben-Dor, S.,  
616 Gottlieb, H., Hernandez, A., Nelson, D. R., Paris, H. S., Tadmor, Y., Burgen, Y.,  
617 Lewensohn, E., Katzin, N., & Schaffer, A. (2016). The biosynthetic pathway of the  
618 nonsugar, high-intensity sweetener mogroside V from *Siraitia grosvenorii*. *Proceedings of*  
619 *the National Academy of Sciences of the United States of America*, 113, 7619–7628.  
620 <https://doi.org/10.1073/pnas.1604828113>.

621 Jaravine, V., Ibraghimov, I. & Orekhov, V. Y. (2006). Removal of a time barrier for high-  
622 resolution multidimensional NMR spectroscopy. *Nature Methods*, 3, 605–607.  
623 <https://doi.org/10.1038/nmeth900>.

624 Kasai, R., Nie, R.-L., Nashi, K., Ohtani, K., Zhou, J., Tao, G.-D., Tanaka, O. (1989). Sweet  
625 cucurbitane glycosides from fruits of *Siraitia siamensis* (chi-zi luo-han-guo), a Chinese  
626 folk medicine. *Agricultural and Biological Chemistry*, 53, 3347–3349.

627 Li, C., Lin, L.-M., Sui, F., Wang, Z.-M., Huo, H.-R., Dai, L., & Jiang, T.-L. (2014). Chemistry  
628 and pharmacology of *Siraitia grosvenorii*: A review. *Chinese Journal of Natural*  
629 *Medicines*, 12, 89–102. [https://doi.org/10.1016/S1875-5364\(14\)60015-7](https://doi.org/10.1016/S1875-5364(14)60015-7).

630 Li, D., Ikeda, T., Matsuoka, N., Nohara, T., Zhang, H., Sakamoto, T., & Nonaka, G. I. (2006).  
631 Cucurbitane glycosides from unripe fruits of Lo Han Kuo (*Siraitia grosvenori*). *Chemical*  
632 *and Pharmaceutical Bulletin*, 54, 1425–1428. <https://doi.org/10.1248/cpb.54.1425>.

633 Li, D., Ikeda, T., Huang, Y., Liu, D. P., Nohara, T., Sakamoto, T., & Nonaka, G. I. (2007).  
634 Seasonal variation of mogrosides in Lo Han Kuo (*Siraitia grosvenori*) fruits. *Journal of*  
635 *Natural Medicines*, 61, 307–312. <https://doi.org/10.1007/s11418-006-0130-7>.

636 Luo, Z., Shi, H., Zhang, K., Qin, X., Guo, Y., & Ma, X. (2016). Liquid chromatography with  
637 tandem mass spectrometry method for the simultaneous determination of multiple sweet  
638 mogrosides in the fruits of *Siraitia grosvenorii* and its marketed sweeteners. *Journal of*  
639 *Separation Science*, 39, 4124–4135. <https://doi.org/10.1002/jssc.201600563>.

640 Makapugay, H. C., Nanayakkara, N. P. D., Soejarto, D. D., & Kinghorn, A. D. (1985). High-  
641 performance liquid chromatographic analysis of the major sweet principle to Lo Han Kuo  
642 fruits. *Journal of Agricultural and Food Chemistry*, 33, 348–350.  
643 <https://doi.org/10.1021/jf00063a007>.

644 Niu, B., Ke, C.-Q., Li, B.-H., Li, Y., Yi, Y., Luo, Y., Shuai, L., Yao, S., Lin, L.-G., Li, J., &  
645 Ye, Y. (2017). Cucurbitane glycosides from the crude extract of *Siraitia grosvenorii* with  
646 moderate effects on PGC-1 $\alpha$  promoter activity. *Journal of Natural Products*, 80, 1428–  
647 1435. <https://doi.org/10.1021/acs.jnatprod.6b01086>.

648 Pawar, R. S., Krynitsky, A. J., & Rader, J. I. (2016). Sweeteners from plants – with emphasis  
649 on *Stevia rebaudiana* (Bertoni) and *Siraitia grosvenorii* (Swingle). *Analytical and*  
650 *Bioanalytical Chemistry*, 405, 4397–4407. <https://doi.org/10.1007/s00216-012-6693-0>.

651 Prakash, I., & Chaturvedula, V. S. P. (2014). Additional new minor cucurbitane glycosides  
652 from *Siraitia grosvenorii*. *Molecules*, 19, 3669–3680.  
653 <https://doi.org/10.3390/molecules19033669>.

654 Qing, Z.-X., Zhao, H., Tang, Q., Mo, C.-M., Huang, P., Cheng, P., Yang, P., Yang, X.-Y., Liu,  
655 X.-B., Zheng, Y.-J., & Zeng, J.-G. (2017). Systematic identification of flavonols, flavonol  
656 glycosides, triterpene and siraic acid glycosides from *Siraitia grosvenorii* using high-  
657 performance liquid chromatography/quadrupole-time-of-flight mass spectrometry

658 combined with a screening strategy. *Journal of Pharmaceutical and Biomedical Analysis*,  
659 138, 240–248. <https://doi.org/10.1016/j.jpba.2017.01.059>.

660 Schleucher, J., Schwendinger, M., Sattler, M., Schmidt, P., Schedletzky, O., Glaser, S. J.,  
661 Sørensen, O. W. & Griesinger, C. (1994). A general enhancement scheme in heteronuclear  
662 multidimensional NMR employing pulsed field gradients. *Journal of Biomolecular NMR*,  
663 4, 301–306. <https://doi.org/10.1007/BF00175254>.

664 Shaw, A. A., Salaun, C., Dauphin, J.-F., & Ancian, B. (1996). Artifact-free PFG-enhanced  
665 double-quantum-filtered COSY experiments. *Journal of Magnetic Resonance, Series A*,  
666 120, 110–115. <https://doi.org/10.1006/jmra.1996.0105>.

667 Shen, Y., Lin, S., Han, C., Zhu, Z., Hou, X., Long, Z., & Xu, K. (2014). Rapid identification  
668 and quantification of five major mogrosides in *Siraitia grosvenorii* (Luo-Han-Guo) by  
669 high-performance liquid chromatography-triple quadrupole linear ion trap tandem mass  
670 spectrometry combined with microwave-assisted extraction. *Microchemical Journal*, 116,  
671 142–150. <https://doi.org/10.1016/j.microc.2014.04.014>.

672 Soejarto, D. D., Addo, E. M., & Kinghorn, A. D. (2019). Highly sweet compounds of plant  
673 origin: From ethnobotanical observations to wide utilization. *Journal of*  
674 *Ethnopharmacology*, 243, 112056. <https://doi.org/10.1016/j.jep.2019.112056>.

675 United States Pharmacopeial Convention (2018). Food Chemicals Codex (11th ed.). Rockville,  
676 MD: The United States Pharmacopeial Convention, USP (pp. 817–818).

677

678